The non-equilibrium charge screening effects in diffusion-driven systems with pattern formation

V. N. Kuzovkov,[1,a)] E. A. Kotomin,[1] and M. Olvera de la Cruz[2,b)]
[1]*Institute for Solid State Physics, University of Latvia, 8 Kengaraga Street, LV – 1063 RIGA, Latvia*
[2]*Department of Materials Science and Engineering, Northwestern University, Evanston, Illinois 60208, USA*

(Received 13 June 2011; accepted 23 June 2011; published online 20 July 2011)

The effects of non-equilibrium charge screening in mixtures of oppositely charged interacting molecules on surfaces are analyzed in a closed system. The dynamics of charge screening and the strong deviation from the standard Debye-Hückel theory are demonstrated via a new formalism based on computing radial distribution functions suited for analyzing both short-range and long-range spacial ordering effects. At long distances the inhomogeneous molecular distribution is limited by diffusion, whereas at short distances (of the order of several coordination spheres) by a balance of short-range (Lennard-Jones) and long-range (Coulomb) interactions. The non-equilibrium charge screening effects in transient pattern formation are further quantified. It is demonstrated that the use of screened potentials, in the spirit of the Debye-Hückel theory, leads to qualitatively incorrect results. © *2011 American Institute of Physics*. [doi:10.1063/1.3613622]

I. INTRODUCTION

The role of electrostatic interactions in surface pattern formation and phase separation phenomena is crucial in various technological processes and scientific problems.[1,2] Moreover, most biological systems and many bio-inspired materials consist of mixtures of oppositely charged macroions that segregate into ionic complexes or complex coacervates.[3] Many applications such as coatings for medical devices[2] and implant materials[4] rely on understanding the self-organization of these coacervates on surfaces. Adhesive proteins of marine organism as well as mixtures of oppositely charged hydrophilic synthetic polyelectrolytes, for example, segregate into wet phases rich in oppositely charged macroions.[5–8] The physical properties of these coacervates allow the concentration and spread of adhesive proteins over selected surfaces without loss to the surrounding water.[9] Therefore, ionic complexation on surfaces has strong potential to generate bio-inspired adhesives.[4] In general, the complexation of nearly electroneutral mixtures of oppositely charged molecules depends on their charge densities and ionic concentrations.[6] Adhesive proteins lack secondary structure,[9] which suggests that simple van der Waals or symmetric dispersion forces and electrostatic interactions can describe successfully these ionic complexes.

The competing long- and short-range interactions in mixtures of oppositely charged molecules on surfaces lead to interesting equilibrium patterns.[10,11] The ordering kinetics of diffusive, oppositely charged molecules on surfaces, however, are not well understood.[12] If the energy of forming the ionic complexes is larger than the thermal energy, the resulting structures may not be in thermodynamical equilibrium: this explains the dynamical properties of coacervates[6] as well as the inhomogeneous coatings of oppositely charged functionalized nanoparticles.[13] In fact, as discussed in this work, even in the case of weak van der Waals interactions competing with long-range electrostatic effects, the expected equilibration is difficult to achieve on surfaces on the typical experimental time scale.

Here we consider spatial effects on the kinetics of ordering processes due to the long-range interactions between oppositely charged molecules diffusing on surfaces. In the kinetic process of developing short- and long-range ionic correlations, non-equilibrium charge screening occurs due to different time scales that naturally develop during the ordering process.

II. THEORETICAL APPROACH

Charge screening effects are generally analyzed using the standard Debye-Hückel (DH) model. The DH method is based on the self-consistent solution of the Poisson equation aimed at finding the electrostatic potential $\phi(r)$ for a spatial distribution of particles (which, in turn, depends on the potential), and is useful for computing static particle correlation functions in many physical limits. When a probe charge e_i is placed into the system of oppositely charged molecules (particles) A and B with charges $e = e_A = -e_B$, the potential of the induced field $\phi_i(r)$ differs from a probe potential $\phi_i^0(r)$ by the *screening factor* $Q_i(r)$: $\phi_i(r) = Q_i(r)\phi_i^0(r)$. In particular, under some conditions,[14] the screening factor for the 3D system is $Q_i(r) = Q^{DH}(r) = \exp(-r/r_{DH})$, where r_{DH} is the DH radius or screening length, defined by actual system parameters. The main effect is that each charged molecule is surrounded by a cloud of oppositely charged molecules with concentration that exceeds the average molecule concentration. At distances larger than the cloud size $r > r_{DH}$, the Coulomb interaction can be neglected.

Such a model is valid for ideal gases where charges (electrons or point particles) are very mobile and rapidly

a)Electronic mail: kuzovkov@latnet.lv.
b)Electronic mail: m-olvera@northwestern.edu.

equilibrate. However, this is often not the case for electrolytes or condensed matter where the particles have a non-zero size and/or short-range interactions. Moreover, in soft and condensed matter, the molecules are characterized by partial diffusion coefficients, D_A and D_B,[15,16] which could differ by orders of magnitude. Molecular diffusion is quite slow and thus molecular distribution is usually *far from equilibrium*. The effects of ion sizes[17] and other ion-specific effects have been extensively studied,[18] and are known to generate static correlation with modified long-range interactions (such as modified DLVO or Yukawa potentials by nonlinear effects in colloids[19]) and other nonlinear DH effects that lead to oscillatory correlation functions.[20] The kinetic effects, however, on the dynamic correlation functions of ionic mixtures have not been analyzed, even for the simplest symmetrical case of $D_A = D_B$ and of equal component ion sizes.

Non-equilibrium effects arise in systems where spatial density fluctuations are governed by particle diffusion. At a finite time t, the structure at long distances from a probe charge remains non-equilibrium, and the screening factor becomes consequently time-dependent, $Q_i(r,t)$. In the general case of asymmetric diffusion, $D_A \neq D_B$, there are *two* different screening factors, $Q_A(r,t) \neq Q_B(r,t)$. Along with assumption of the equilibrium distribution, there exists an additional problem of the Poisson-Boltzmann equation regarding its neglect of short-range particle interactions. This creates a serious problem since such system of classical particles with purely electrostatic interactions is known to be unstable. Indeed, neglecting short-range potentials raises doubts about the accuracy of the DH screening factor $Q^{DH}(r)$ at *short* distances, $r < r_{DH}$.

In order to improve the standard DH theory, we consider here a microscopic kinetic model for two oppositely charged, interacting components based upon computing the *many-point-particle densities*.[12,15,16] The exact set of the coupled kinetic equations is similar to the Bogoliubov-Born-Green-Kirkwood-Yvon hierarchy[14] in statistical physics. In a closed system with two types of particles (molecules) without reaction, the total number of particles remains constant. The first equation set of a system of coupled equations describes the radial distribution functions (or joint correlation functions): for similar particle types: $g_{AA}(r,t)$ and $g_{BB}(r,t)$, and for dissimilar particles: $g_{AB}(r,t)$ where r is the relative distance between any two particles (A or B). These functions describe the spatial distribution of pairs AA, BB, and AB.

The general structure of the nonlinear equations $g_{ij}(r,t)$ takes the form,[12]

$$\frac{\partial g_{ij}(r,t)}{\partial t} = D_{ij}\nabla\left[\nabla g_{ij}(r,t) + \frac{g_{ij}(r,t)}{k_B T}\nabla W_{ij}(r,t)\right], \tag{1}$$

where $i, j = A, B$. These equations describe the particle diffusion drift in various potentials of mean force $W_{ij}(r,t)$ that are, in turn, functionals of the correlation functions. The quantities D_{ij} are coefficients related to the partial diffusion coefficients of particles, D_A and D_B, by $D_{ij} = D_i + D_j$.[12] At long distances, the correlation functions tend to unity (random or Poisson distribution): $g_{ij}(\infty,t) = 1$.[15,16] Positive or negative deviations from unity indicate aggregation or depletion of particles, respectively. The set of coupled kinetic equations is solved numerically by discretizing them and by using standard recursive procedure for nonlinear terms.[12]

Let us assume in our equilibration kinetics analysis that our system of oppositely charged molecules at the interface (2D) is initially well stirred, and the temperature T is constant. Since the joint correlation functions characterize only the *relative* correlations in particle distribution, we performed additionally their analysis using the reverse Monte Carlo (RMC),[12,21] which permits us to learn about pattern formation effects through snapshots of particles distribution in real space. The same is true for the screening factors.

To simulate the short-range van der Waals interactions, we use the commonly used classical 6-12 Lennard-Jones potential,

$$U(r) = 4U_0\left[\left(\frac{r_0}{r}\right)^{12} - \left(\frac{r_0}{r}\right)^{6}\right]. \tag{2}$$

Keeping in mind our interest in studying the effects of diffusion asymmetry (additional parameter), we minimize a number of free parameters assuming U_0 and r_0 are the same for similar and dissimilar pairs.[22] The Lennard-Jones potential describes particle repulsion at short distances, $r < r_c = 2^{1/6}r_0$, due to finite particle sizes where the force field $F(r) = -\partial U(r)/\partial r$ is positive, and particle attraction at larger distances, $r > r_c$, where the force field is negative. We assume same repulsion effects for both similar and dissimilar molecular pairs but—following commonly used model[10,12,22]—truncate the dissimilar pair attraction at $r > r_c$. As a result, A- and B-type molecules repel each other without Coulomb interactions, and molecules of the same type attract each other and can thus aggregate. Additional inclusion of Coulomb interactions, as we show below, stabilizes the system of dissimilar-type molecules and allows for pattern formation.

The aforementioned potential is characterized by two parameters: the length r_0 and the energy denoted by U_0 that correspond to the given temperature $T_0 = U_0/k_B$. It is convenient to use *dimensionless* parameters for both temperature, $\theta = T/T_0$, and for the relative magnitude between the Coulomb and Lennard-Jones potentials, $\delta = e^2/\epsilon r_0 k_B T_0$. The total particle density, $n = n_A + n_B$, determines the dimensionless parameter $\eta = nr_0^2$. Asymmetry in the particle diffusion coefficients is described by the parameter $\mu = D_A/(D_A + D_B)$. Lastly, the time unit used is $t_0 = r_0^2/(D_A + D_B)$.

III. RESULTS AND DISCUSSION

We analyze qualitatively the different possible situations: at low temperatures ($\theta < 1$), we find dramatic changes when varying the parameter δ, which controls the ratio of long-range and short-range interactions. When this parameter is small, $\delta < 0.1$, the short-range interactions are predominant[10,12] and dissimilar-type molecules repel each other. In turn, this leads to the segregation of dissimilar-type molecules, where two types of aggregates created by A- and B-type molecules bound to one another at long distances driven by Coulomb forces. As such, unlike the

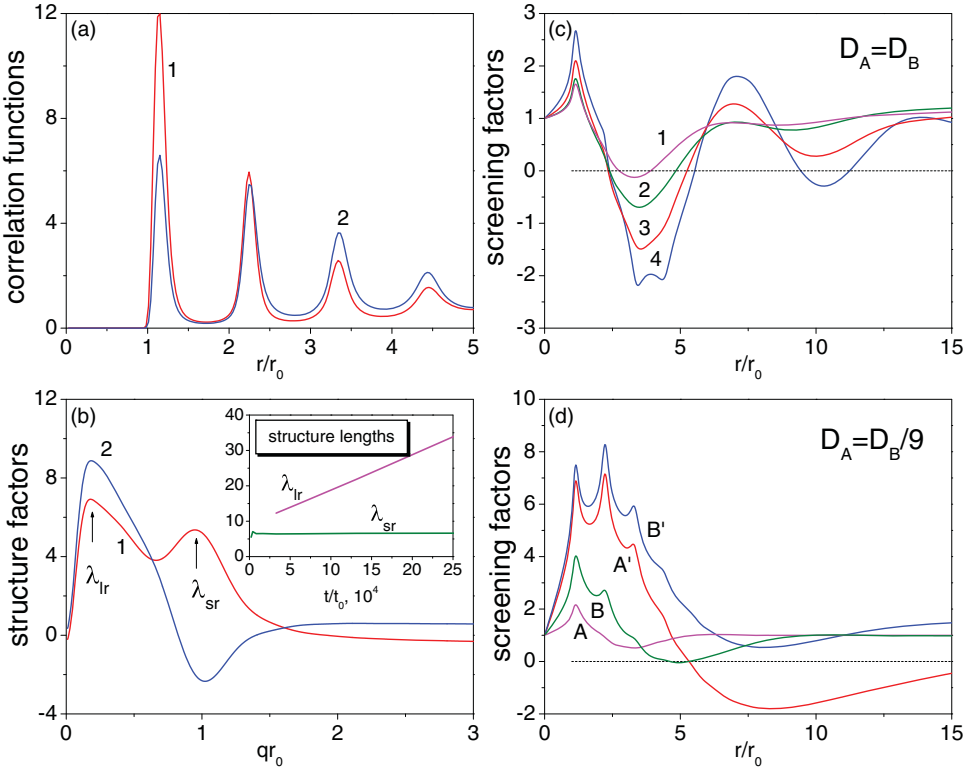

FIG. 1. Ionic binary systems with Lennard-Jones and Coulomb interactions at low temperatures for intermediate density, $\eta = 0.4$. Parameter are: (a)–(c) $\delta = 0.35$, $\theta = 0.35$ for symmetric diffusion, and (d) 0.05, $\theta = 0.40$ for asymmetric diffusion. Curves are shown for times t/t_0: (a) and (b) 2^{18}; (c) 2^{12} (1), 2^{14} (2), 2^{16} (3), and 2^{18} (4); (d) 2^{12} (A, B) and 2^{18} (A', B').

classical DH model where the screening factor was determined by re-arrangement of individual particles (charges) according to the Boltzmann distribution, we observe here the re-arrangement of large molecular aggregates (*super-particles*). Because these super-particles are very large, their ordering also requires considerable time. Therefore, the ordering kinetics is not steady-state since aggregate formation and growth are both very slow processes, which starts with nucleation of many small aggregates (local ordering) followed by the further growth of larger aggregates at the expense of smaller ones (intermediate-scale ordering).

Faster ordering process is characterized by the intermediate values of $0.1 < \delta < 0.5$. An oscillatory behavior is observed here for the correlation functions, which is typical for condensed matter with ordering within several spheres surrounding a chosen particle. Further increase in the magnitude of Coulomb interactions relative to van der Waals ($\delta > 0.5$) results in the formation of smaller clusters made of similar-type molecules, such as dimers and trimers, held together by electrostatic interactions. Thus, a system exhibiting pattern formation is characterized by the emergence of *several* structural scales: (i) the size of the super-particles, (ii) the size of recurring (repeating) elements constituting the pattern (consisting of several super-particles), and lastly, (iii) the average size of the whole pattern. Development of each of these three length scales requires three quite different characteristic ordering (relaxation) time scales.

To support the above point, let us first discuss the results of the numerical calculations for the joint correlation functions, as time evolves, regarding the symmetric case ($D_A = D_B$) shown in Fig. 1(a) for intermediate δ values and low temperatures; the quantities $g_{AA}(r,t) = g_{BB}(r,t)$ and $g_{AB}(r,t)$ are denoted by the indices 1 and 2. The relaxation process at short distances is very fast: the results for two very different times are practically identical. This means that the repeating element of the pattern can be created very quickly. In contrast, creating the patterns of a large size is a very slow process. We quantify the relaxation of these different length scales, λ_{sr} and λ_{lr} as defined in Fig. 1(b), by computing the *partial structure factors*,[23] $S_{AA}(q,t) = S_{BB}(q,t)$ and $S_{AB}(q,t)$, denoted by 1 and 2, respectively, in Fig. 1(b). In each case, there are two extrema at $(qr_0)_{sr} = 2\pi/\lambda_{sr}$ and $(qr_0)_{lr} = 2\pi/\lambda_{lr}$. The quantity $(qr_0)_{sr}$ is mainly time-independent, while $(qr_0)_{lr}$ (at lower qr_0 values) changes with time. The kinetic process is quantified in Fig. 1(b) (inset), where we plot λ_{sr} and λ_{lr} as functions of time. The maximum for λ_{sr} remains the same (in our case $\lambda_{sr} \approx 7$) with time except at very short times. On the other hand, the long-range maximum λ_{lr} grows linearly with time.

In Fig. 2(a) we show the typical snapshot of the structure of the non-equilibrium system (with same parameters as those in Fig. 1(a)). These snapshots were generated using the above-mentioned RMC. As one can see, the pattern is constructed by the alternation of super-particles (small aggregates), each consisting of A- and/or B-type molecules. The size of a repeating element in the pattern is of the order of λ_{sr}. On the other hand, the scale factor λ_{lr} characterizes the average size of dendridic-type clusters, which are porous-like structures of

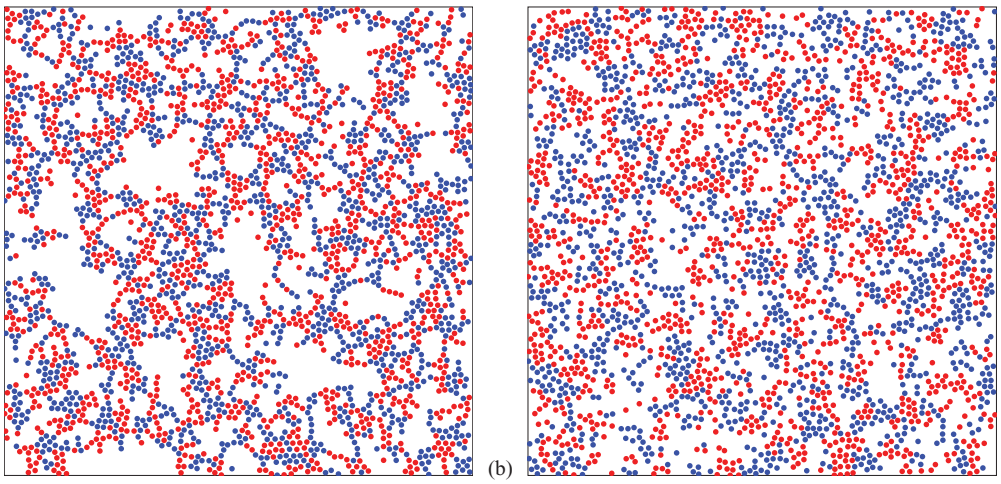

FIG. 2. Characteristic structure snapshots obtained using the RMC: (a) corresponds to the structure factors in Fig. 1(b), whereas (b) the structure factors in Fig. 3(a), curves (3,3′).

low density: as the snapshot is computed at low temperature θ, which is equivalent to having strong interactions, it results in a nearly frozen structure that cannot relax to a compact aggregate (in fact, we observe a lamellar structure similar to that detailed in Ref. 10).

Although the steady-state solution associated with the segregation process is independent of the diffusion coefficients of individual molecules, the magnitude and evolution of non-equilibrium screening effects strongly depend on the ratio D_A/D_B. We first discuss the symmetric case where $D_A = D_B$. We plot in Fig. 1(c) the screening factor at several time values, using the same parameters as those in Figs. 1(a) and 1(b). One can see immediately a strong deviation from the DH theory, where the screening factor is supposed to drop down monotonically from unity to zero. Instead, this plot shows a strong degree of *overcharging* (charge amplification) at small r/r_0-values due to the short-range van der Waals attraction between similar-type molecules. The screening factor then oscillates between charge amplification and charge reversal as the quantity r/r_0 increases. The amplitude of these oscillations increases as a function of time, and they shift to longer r/r_0-values as the clustering becomes more pronounced (the equilibrium structure tends to the lamellar type).

Let us consider now the effects of diffusion asymmetry by plotting the screening factor at two different time values for $D_A = D_B/9$, which is shown in Fig. 1(d) for θ values slightly higher than those for Figs. 1(a)–1(c). Both molecule types exhibit charge amplification. However, the faster molecules do not show exhibit charge reversal as time evolves in Fig. 1(d); that is, their clusters are not covered with oppositely charged molecules during segregation. Meanwhile, the slower diffusive molecules, as time evolves, are surrounded by oppositely charged particles, leading to a a faster local charge inversion.

The self-consistent solution regarding the relationship between the electrostatic potential and the joint correlation functions is a very non-trivial mathematical problem. In the commonly used approximation,[13,24,25] the unknown electrostatic potential is replaced with the screened one (e.g., Yukawa potential) with the screening factor $Q(r) = \exp(-r/r_s)$, where r_s is the fitting parameter. As such, such a screened potential is no longer related to the underlying structural parameters of the system (correlation functions). It is believed that this approximation is valid for both liquids and dense gases.

However, we note that the Yukawa potential is short-range in nature. Thus, the introduction of the screened potential eliminates the fundamental difference between the long-range Coulomb and short-range Lennard-Jones potentials that we have been considering. In fact, systems with different type of interactions also exhibit quite different spatial structures. For illustration, Fig. 3(a) demonstrates the same ionic binary systems, at a higher temperature, $\theta = 0.5$, and for a weak electrostatic potential. An increase in temperature leads to the transition from an ordered (crystalline) to disordered (liquid-like) structure, for which the DH theory intuitively should be more aptly applicable. As we show below, this turns out to be not the case.

A comparison of Figs. 3(a) and 3(b) illustrates the fundamental difference in the calculated structural factors. In particular, the partial structural factors $S_{AA}(q,t) = S_{BB}(q,t)$ in Fig. 1(b) reveal two maxima, whereas only one maximum is seen in Fig. 3(a). In other words, the two systems reveal two different types of pattern formation. The typical snapshot of the structure corresponding to the case (3.3′) in Fig. 3(a) and obtained using the RMC is shown in Fig. 2(b). Snapshots for other cases are similar: disordered (liquid-like) structure with the trend to form loose aggregates made of similar-type molecules.

The case of (1,1′) in Fig. 3(a) corresponds to the limiting scenario of $\delta = 0$ for which only the short-range Lennard-Jones interaction is present, while in all other cases the long-range interactions are included. Analysis of the relevant structural factors in Fig. 3(a) allows us to observe their fundamental difference. Without Coulomb interactions, the structure factor $S_{AB}(q,t)$ has a minimum at small wavenumber q [curve (1′)]. Otherwise, the inclusion of Coulomb interactions leads to the appearance of *maxima* [curves (2′,3′,4′)] in

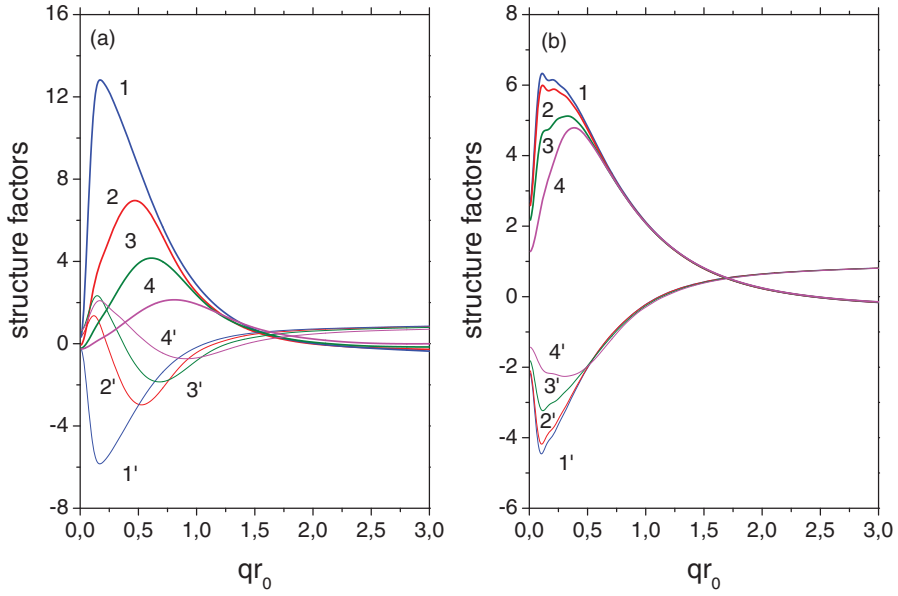

FIG. 3. The structure factors $S_{AA}(q,t) = S_{BB}(q,t)$ [curves (1-4)] and $S_{AB}(q,t)$ [curves (1′–4′)] for ionic binary systems at intermediate temperature, $\theta = 0.5$, for intermediate density, $\eta = 0.4$. Curves are shown for time $t/t_0 = 2^{18}$. (a) The result of the self-consistent solution properly taking into account the spatial correlations of molecules. Parameter δ is: (1) 0.0, (2) 0.05, (3) 0.10, and (4) 0.20; (b) The simplified solution using the screened (Yukawa) potential for the case (3.3′), i.e., $\delta = 0.10$. The screening length r_s/r_0: (1) 1, (2) 2, (3) 4, and (4) 8.

the same q-region. As small q-values correspond to large distances, this observation implies that charged systems exhibit characteristic Coulomb peculiarities in the relative distribution of AB-pairs at such large distances. A similar (but more pronounced) maximum is also observed at low temperatures (Fig. 1(b)).

For comparison, the results pertaining to the approximate treatment based on the aforementioned Yukawa potential are presented in Fig. 3(b) with various fitting parameters. It is obvious that all cases in Fig. 3(b) are qualitatively close only to the curves (1.1′) found in Fig. 3(a) that correspond to the lack of long-range interactions. The aforementioned Coulomb peculiarities at small wavenumbers are also absent here. Note that the structure visualization using the RMC (Fig. 2(b)) shows only similar-type molecular aggregation that occurs with and without Coulomb interactions. On the other hand, the previously discussed Coulomb peculiarities in the structure factors arise due to the spatial rearrangement of such aggregates at *long* distances. Therefore, the use of the screened potentials, in the spirit of the equilibrium DH theory, leads to qualitatively incorrect results.

IV. CONCLUSIONS

We have shown here that equilibration processes in a closed system with two types of oppositely charged molecules, in the presence of short-range interactions that generally induce local ordering, do not achieve the DH-limit characteristic of steady-state molecular distributions. In fact, the non-equilibrium charge screening factors are determined by both process kinetics (anomalously long ordering times at large length scales) and short-range interactions (lamellar-like patterns). In all the different cases considered in this work, the structure of the ionic cloud surrounding a probe charge is non-trivial and *qualitatively differs* from the expected in the standard DH approach.

Furthermore, we found two length scales governing the pattern formation process. The short length scale (formation of seeding elements in future pattern) is rapidly established with respect to time. Meanwhile, the long length scale grows linearly in time at intermediate time values, which is characteristic of percolated dendritic (fractal-like) growth in two dimensions.[26]

These results explain some of the properties of bio-inspired complex coacervates,[9] as well as of inhomogeneous functionalized nanoparticle coatings.[2,13] In experiments of protein and the polysaccharide coacervates,[27] for example, it is observed that the diffusion of the macroions in ionic complexes is the slowest when the electrostatic interactions are at maximum, and that the protein and the polysaccharide moved independently in the coacervate phase. Moreover, the existence of intra- and inter-molecular aggregates, where the small aggregates are much less dynamic, is well documented.[28] These experimental facts support our overall observations.

ACKNOWLEDGMENTS

We thank the DDR&E and the AFOSR under Award No. FA9550-10-1-0167 and the NERC, which is an EFRC funded by Department of Energy (DOE) under Award No. DE-SC0000989, for financial support, and William Kung for critical reading of this manuscript.

[1]G. Decher, Science **277**, 1232 (1997); E. Sanz, K. A. White, P. S. Clegg, and M. E. Cates, Phys. Rev. Lett. **103**, 255502 (2009); R. Parthasarathy, P. A. Cripe, and J. T. Groves, *ibid.* **95**, 048101 (2005).

[2]K. V. Tretiakov, K. J. M. Bishop, B. Kowalczyk, A. Jaiswal, M. A. Poggi, and B. A. Grzybowski, J. Phys. Chem. A **113**, 3799 (2009); S. K. Smoukov, K. J. M. Bishop, B. Kowalczyk, A. M. Kalsin, and B. A. Grzybowski, J. Am. Chem. Soc. **129**, 15623 (2007).
[3]E. Raspaud, M. Olvera de la Cruz, J.-L. Sikorav, and F. Livolant, Biophys. J. **74**, 381 (1998); D. A. Walker, B. Kowalczyk, M. Olvera de la Cruz, and B. A. Grzybowski, Nanoscale **3**, 1316 (2011).
[4]H. Lee, B. P. Lee, and P. B. Messersmith, Nature (London) **448**, 338 (2007); D. S. Hwang, J. H. Waite, and M. Tirrell, Biomaterials **31**, 1080 (2010).
[5]H. Zhao, C.-J. Sun, R. J. Stewart, and J. H. Waite, J. Biol. Chem. **280**, 42938 (2005).
[6]C. G. de Kruif, F. Weinbreck, and R. de Vries, Curr. Opin. Colloid Interface Sci. **9**, 340 (2004).
[7]A. Kudlay and M. Olvera de la Cruz, J. Chem. Phys. **120**, 404 (2004); J. Lee, Y. O. Popov, and G. H. Fredrickson, J. Chem. Phys. **128**, 224908 (2008); I. I. Potemkin and V. V. Palyulin, Phys. Rev. E **81**, 041802 (2010).
[8]R. Chollakup, W. Smitthipong, C. D. Eisenbach, and M. Tirrell, Macromolecules **43**, 2518 (2010); E. Spruijt, A. H. Westphal, J. W. Borst, M. A. Cohen Stuart, and J. van der Gucht, *ibid.* **43**, 6476 (2010).
[9]D. S. Hwang, H. Zeng, A. Srivastava, D. V. Krogstad, M. Tirrell, J. N. Israelachvili, and J. H. Waite, Soft Matter **6**, 3232 (2010).
[10]S. M. Loverde, F. J. Solis, and M. Olvera de la Cruz, Phys. Rev. Lett. **98**, 237802 (2007).
[11]L. Assoud, R. Messina, and H. Lowen, Euro. Phys. Lett. **89**, 36001 (2010).
[12]V. N. Kuzovkov, E. A. Kotomin, G. Zvejnieks, and M. Olvera de la Cruz, Phys. Rev. E **82**, 021602 (2010).
[13]I. Lagzi, B. Kowalczyk, and B. A. Grzybowski, J. Am. Chem. Soc. **132**, 58 (2010).
[14]R. Balescu, *Equilibrium and Non-equilibrium Statistical Mechanics* (Wiley, New York, 1975).
[15]E. A. Kotomin and V. N. Kuzovkov, Rep. Prog. Phys. **55**, 2079 (1992).
[16]E. A. Kotomin and V. N. Kuzovkov, *Modern Aspects of Diffusion-Controlled Reactions: Cooperative Phenomena in Bimolecular Processes* (Elsevier, North Holland, Amsterdam, 1996).
[17]G. I. Guerrero-Garcia, E. Gonzalez-Tovar, and M. Olvera de la Cruz, Soft Matter **6**, 2056 (2010).
[18]J. Zwanikken and M. Olvera de la Cruz, Phys. Rev. E **82**, 050401 (2010).
[19]S. Alexander, P. M. Chaikin, P. Grant, G. J. Morales, and P. Pincus, J. Chem. Phys. **80**, 5776 (1984); L. Belloni, *ibid.* **85**, 519 (1986).
[20]R. Kjellander and D. J. Mitchell, J. Chem. Phys. **101**, 603 (1994); P. González-Mozuelos, M. S. Yeom, and M. Olvera de la Cruz, Eur. Phys. J. E **16**, 167 (2005).
[21]R. L. McGreevy and L. Pusztai, Mol. Simul. **1**, 359 (1988); R. L. McGreevy, J. Phys.: Condens. Matter **13**, 877 (2001).
[22]D. Frenkel and B. Smit, *Understanding Molecular Simulation* (Academic, New York, 2001).
[23]T. E. Faber and J. M. Ziman, Philos. Mag. **11**, 153 (1965).
[24]M.-G. Song, K. J. M. Bishop, A. O. Pinchuk, B. Kowalczyk, and B. A. Grzybowski, J. Phys. Chem. C **114**, 8800 (2010).
[25]A. M. Kalsin, M. Fialkowski, M. Paszewski, S. K. Smoukov, K. J. M. Bishop, and B. A. Grzybowski, Science **312**, 420 (2006).
[26]H. Brune, C. Romalnczyk, H. Roder, and K. Kern, Nature (London) **369**, 469 (1994).
[27]F. Weinbreck, H. S. Rollema, R. H. Tromp, and C. G. de Kruif, Langmuir **20**, 6389 (2004).
[28]M. Girard, C. Sanchez, S. I. Laneuville, S. L. Turgeon, and S. F. Gauthier, Colloids Surf., B **35**, 15 (2004).